

---

**Future projections of false spring events in the eastern part of the Baltic Sea region**

**Laurynas Klimavičius\*, Egidijus Rimkus**


Klimavičius, L., Rimkus, E. 2025. Future projections of false spring events in the eastern part of the Baltic Sea region. *Baltica* 38 (2), 160–173. Vilnius. ISSN 1648-858X.

Manuscript submitted 12 May 2025 / Accepted 10 November 2025 / Available online 27 November 2025

© Baltica 2025

**Abstract.** In recent decades, rising winter and spring temperatures have led to an earlier onset of the growing season. However, this shift is often accompanied by false spring (FS) events – situations when the last spring frost (LSF) occurs after the start of the growing season (SGS). This study evaluates future changes in the recurrence and intensity of FS events in the eastern part of the Baltic Sea region. The SGS and LSF dates for each grid cell within the study area for each year were determined to identify FS events. An FS event was recorded when LSF occurred later than the SGS date. The intensity of FS events was assessed using growing degree days (GDD) accumulated until the event. Future projections were generated using five CMIP6 models (CanESM5, ACCESS-CM2, GFDL-CM4, MPI-ESM1-2-LR, and NorESM2-MM), two SSP scenarios (SSP2-4.5 and SSP5-8.5), and data obtained from the NASA NEX-GDDP-CMIP6 dataset. The period from 1995 to 2014 was used as the baseline, and projections were made for the years 2041–2060 and 2081–2100. Analysis showed that SGS and LSF dates are projected to shift significantly earlier under all models and scenarios. However, FS recurrence projections are less consistent. Most models indicate a decline in FS events by mid-century, while forecasts for 2081–2100 are mixed – two models suggest an increase, while the other three suggest a decrease. The mean GDD sum accumulated until the FS event increases only when the frequency of FS events is projected to rise, suggesting that future FS events may be more intense.

**Keywords:** *spring frost; growing season; compound climate events; Baltic States*

Laurynas Klimavičius\* ([laurynas.klimavicius@chgf.vu.lt](mailto:laurynas.klimavicius@chgf.vu.lt)),  <https://orcid.org/0009-0002-0243-1421>; Egidijus Rimkus  
Institute of Geosciences, Vilnius University, Vilnius, Lithuania

\*Corresponding author

---

## INTRODUCTION

In recent decades, under warming climate conditions, due to increased air temperatures in winter and spring months, the growing season in various regions of the Northern Hemisphere has been starting increasingly earlier (Jeong *et al.* 2011; Allstadt *et al.* 2015; Xia *et al.* 2015; Zhu *et al.* 2019; Wang *et al.* 2021). This results in a longer growing season and may offer potential benefits for the agricultural sector (Peltonen-Sainio *et al.* 2009; Peterson, Abatzoglou 2014; Grigorieva *et al.* 2023). However, it was already observed in the early 1980s that despite the earlier start of the growing season due to climate change, the risk of spring frosts does not decrease and may even increase (Cannell, Smith 1986), creating favour-

able conditions for a compound climate event known as a ‘false spring’ (Zscheischler *et al.* 2020). A false spring occurs when unusually high temperatures in early spring trigger the onset of vegetation growth, followed by a cold period during which the daily minimum air temperature drops below 0 °C (Ault *et al.* 2013; Chamberlain *et al.* 2019).

False spring events primarily affect fruit trees (Jarzyna 2021; Bateman 2022; Bosdijk *et al.* 2024). During the leaf emergence and blooming stages of fruit trees, frosts are especially dangerous (Rodrigo 2000; Crassweller 2024) and can result in the loss of a large part or even the entirety of the harvest, causing economic losses that may reach several billion euros (Faust, Herbold 2017; Ma *et al.* 2019; Bateman 2022). However, these compound climate events

cause harm not only to plants. The indirect negative impacts of false springs are also felt in other areas. They can threaten ecosystem services, making information about these events and their potential effects and damages important for various institutions, such as national parks (Monahan *et al.* 2016; Martinuzzi *et al.* 2019).

False spring events can also indirectly affect various ecosystems – for example, by disrupting bird migration cycles and reducing food availability, especially when accompanied by snowfall or ice formation (Bateman 2022). The development of leaves and flowers stimulates the flow of sap, nectar, and nutrients in plants. It provides shelter and food for various organisms. A false spring event disrupts this entire system, causing harm to various plant and animal species. For example, repeated false spring events over several consecutive years contributed to the extinction of Edith's checkerspot butterfly species in the Sierra Nevada in the late 20<sup>th</sup> century (Grossman 2014).

Various climatic, geographic, and biological factors determine the recurrence, intensity, and potential adverse effects of false spring events. The primary geographic factors are the distance from large water bodies (seas, oceans) and terrain. Also critical are the average spring air temperature and prevailing atmospheric circulation patterns and anomalies (Ma *et al.* 2019; Cook *et al.* 2020; Chamberlain *et al.* 2021; Hájková *et al.* 2023). Nevertheless, plant species are the most critical factor in determining the strength of a false spring (Ball *et al.* 2011; Chamberlain *et al.* 2019; Baumgarten *et al.* 2023). A plant's cold tolerance depends on its species – some are damaged when temperatures fall below  $-2.2\text{ }^{\circ}\text{C}$ , while others can withstand temperatures below  $-8.5\text{ }^{\circ}\text{C}$  (Chamberlain *et al.* 2021). Another critical factor dependent on species is a plant's ability to recover after experiencing a false spring event (Augspurger 2013; Baumgarten *et al.* 2023; Muffler *et al.* 2024). The unequal impact of these events on different species and their differing abilities to recover means some plants may gain a competitive advantage (Hufkens *et al.* 2012). This may lead to negative ecological consequences and contribute to shifts or reductions in species distribution ranges (European Climate Risk Assessment 2024).

Various indicators can be used to assess the intensity of false spring (FS) events and their potential impact on plants. One of the most applied measures is the sum of growing degree days (GDD), accumulated until the FS event (Chamberlain, Wolkovich 2023). The GDD assesses the amount of heat required for a plant to reach a particular developmental stage (Miller *et al.* 2001). The method is based on the principle that

plant growth begins once temperatures exceed a certain base threshold, with higher temperatures leading to more rapid plant development (Miller *et al.* 2001; Chun, Changnon 2019). This approach is widely applied to model and predict various phenological stages of plants (McMaster, Wilhelm 1997; Clark, Thompson 2010; Wang *et al.* 2025) and to evaluate the effects of frost on species (Wypych *et al.* 2017; Chun, Changnon 2019; Qiu *et al.* 2024). The use of GDD is appropriate as air temperature is the primary factor directly determining plant development. Another advantage of this method is its practicality – GDD can be applied even in cases where field measurements are not feasible, as it only requires air temperature data (Bhatti *et al.* 2025).

Despite climate warming, the risk of false spring events persists in various regions – the number of frost days during the growing season has increased across 43% of the Northern Hemisphere (Liu *et al.* 2018). The persistence or even rise in the risk of false spring events has also been confirmed in regional studies (Allstadt *et al.* 2015; Jarzyna 2021; Bosdijk *et al.* 2024; Zahradníček *et al.* 2024). Therefore, in recent years, more attention has been paid to assessing changes in the recurrence and intensity of these compound climate events across different parts of the Northern Hemisphere (Ma *et al.* 2019; Martinuzzi *et al.* 2019; Zhu *et al.* 2019; Helali *et al.* 2022; Ford *et al.* 2025). Despite that, no studies have examined future changes in false spring event characteristics in the Baltic States. Only the recurrence and intensity of these compound climate events for the 1950–2022 period have been assessed (Klimavičius, Rimkus 2024). In Poland, more detailed analyses have examined the recurrence and intensity of these events as well as the atmospheric circulation conditions driving their occurrence (Graczyk, Szwed 2020; Koźmiński *et al.* 2023; Nidzgorska-Lencewicz *et al.* 2024; Piotrowski, Bartoszek 2025), but projections for the future have not been made there either.

The primary objective of this study is to evaluate the potential changes in the recurrence and intensity of false spring (FS) events by the middle and end of the 21<sup>st</sup> century in the eastern Baltic Sea region. In the first part of the study, the median dates of the start of the growing season (SGS) and the last spring frost (LSF), FS event recurrence, and the sums of accumulated growing degree days up to the FS event were evaluated for the baseline period of 1995–2014. The second part assesses projected changes in the SGS and LSF dates. The third part discusses projected changes in the recurrence of FS events by the mid and late 21<sup>st</sup> century compared to the baseline period. Finally, the last part is devoted to assessing the projected changes in the intensity of these compound climate events.

## DATA AND METHODS

### Study area

FS events were investigated in the eastern part of the Baltic Sea region (from 53.5° to 59.5° N latitude and from 20° to 28.5° E longitude) (Fig. 1).

The study area is located in the temperate climate zone and, according to the updated Köppen–Geiger climate classification, is classified as the *Dfb* climate type (Beck *et al.* 2018). The eastern part of the Baltic Sea region is situated in an excessive moisture zone – annual precipitation exceeds evaporation (Kilkus, Stonevičius 2011). Therefore, the main factor determining the start of the growing season is air temperature. In the study area, the average spring (March–May) temperature ranges from 3.5 °C in north-western Estonia to 7 °C in the southern part of the study area (Klimavičius, Rimkus 2024).

### Data

FS events were first assessed using ERA5 reanalysis data of daily minimum ( $t_{\min}$ ) and average ( $t_{\text{avg}}$ ) air temperatures for the period from 1995 to 2014, covering the months from January to June. The grid size of the data is  $0.25^\circ \times 0.25^\circ$ . Only grids with more than half of their area covered by land were analysed. The ERA5 reanalysis of air temperature data in mid-latitude areas with a well-developed meteorological station network and without steep elevation changes (e.g., mountains) shows a strong correlation with ground-based observations (McNicholl *et al.* 2022; Velikou *et al.* 2022; Xu *et al.* 2022; Liu *et al.* 2024). This is due to the assimilation of modelled and meteorological station data in creating reanalysis datasets (Hersbach *et al.* 2020).

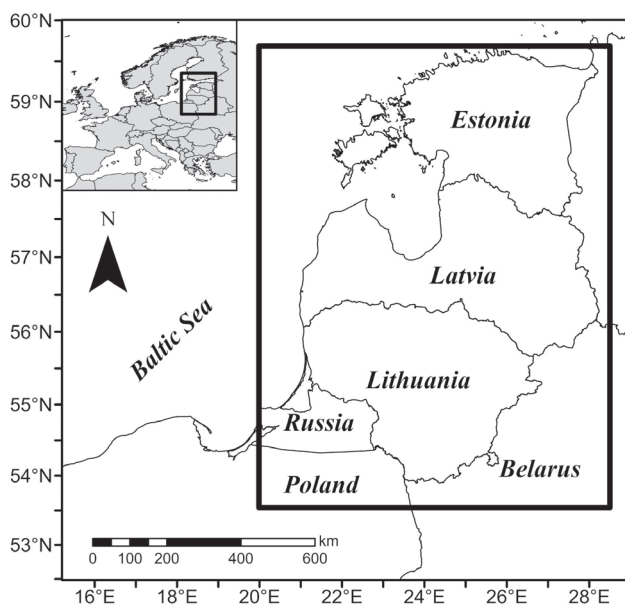


**Fig. 1** The map of the study area

To assess future changes in FS event recurrence,  $t_{\min}$  and  $t_{\text{avg}}$  data from various Coupled Model Inter-comparison Project Phase 6 (CMIP6) general circulation models (GCMs) were used. The data were obtained from the NASA Earth Exchange (NEX) Global Daily Downscaled Projections database (NEX-GDDP-CMIP6), which uses the same  $0.25^\circ \times 0.25^\circ$  grid size as ERA5. This database provides historical data for the period 1950–2014 and climatic projections for the years 2015–2100.

Although the NEX-GDDP-CMIP6 database contains data from 35 different CMIP6 models, only five were selected for this study: CanESM5, ACCESS-CM2, GFDL-CM4, MPI-ESM1-2-LR, and NorESM2-MM (Table 1). These models were chosen based on equilibrium climate sensitivity (ECS), which indicates that the global surface temperature increases when atmospheric  $\text{CO}_2$  concentration is doubled relative to pre-industrial levels (Hausfather 2018). The ECS values of the models used in this study range from 2.5 °C to 5.6 °C (Table 1), thus representing different parts of the sensitivity spectrum (Hausfather 2019).

The NEX-GDDP-CMIP6 database includes data for four Shared Socioeconomic Pathways (SSP) scenarios. However, only two scenarios were used in this study – SSP2-4.5 and SSP5-8.5 – representing medium (radiative forcing increase of 4.5 W/m<sup>2</sup> by 2100) and high (radiative forcing increase of 8.5 W/m<sup>2</sup>) future changes, respectively (Chen *et al.* 2021).

The NEX-GDDP-CMIP6 database was selected for several reasons. First, bias correction was applied during its development to better reflect the conditions at specific locations and align the modelled data more closely with historical climatological data (Thrasher *et al.* 2022). Another issue with using raw CMIP6 GCM data is the low and uneven spatial resolution (typically 80–250 km), which is unsuitable for regional-scale studies (ECMWF 2021). This problem is addressed in the NEX-GDDP-CMIP6 dataset by downscaling all models to a uniform  $0.25^\circ \times 0.25^\circ$  (~25 km) resolution (Thrasher *et al.* 2022). Lastly, this database has been

**Table 1** General circulation models (GCMs) used in the study and their equilibrium climate sensitivity (°C)

Institution and Country of Origin	Model ID	Equilibrium climate sensitivity (°C)
Canadian Centre for Climate Modelling and Analysis, Canada	CanESM5	5.6
CSIRO-BOM, Australia	ACCESS-CM2	4.7
Geophysical Fluid Dynamics Laboratory, USA	GFDL-CM4	3.9
Max Planck Institute for Meteorology, Germany	MPI-ESM1-2-LR	3.0
Norwegian Climate Centre, Norway	NorESM2-MM	2.5



widely used in studies of extreme hydrometeorological events in various regions (Rao *et al.* 2024; Sun *et al.* 2024; Talchabhadel *et al.* 2025), including analyses of spring frosts (Ford *et al.* 2025).

The period from 1995 to 2014 was selected as the baseline period in this study, as it is also used for the same purpose in the IPCC AR6 report (Chen *et al.* 2021). Projections were made for two future periods – mid-century (2041–2060) and end-century (2081–2100).

### Definition of the start of the growing season and the last spring frost

The SGS and LSF dates were determined annually for each grid cell in the study area to identify FS events and assess future changes. Multiple definitions of vegetation season can be found, including the “growing”, “phenological”, “productive”, and “meteorological” seasons (Körner *et al.* 2023). This study adopted the “meteorological season” definition. It identifies the window of opportunity during which meteorological conditions are favourable for growth, and the SGS is determined based on a threshold average daily air temperature and, in some cases, soil moisture values (Körner *et al.* 2023). According to the method proposed by SMHI (SMHI 2025), SGS is defined as the first day of six consecutive days with  $t_{avg} > 5^{\circ}\text{C}$ . The SGS calculations begin on the day of the year when the 10-day running average of air temperature reaches a minimum value. A  $5^{\circ}\text{C}$  threshold has also been used in studies in Northern and Central Europe (Carter 1998; Vitasse, Rebetez 2018; Miś, Tomczyk 2025), as it was found that in Northern European countries, this temperature threshold marks the start of noticeable growth in many plant species (trees, natural vegetation, crops) (Carter 1998).

The LSF is defined as the last day from January to June when the minimum temperature ( $t_{min}$ ) drops below  $0^{\circ}\text{C}$ . At this temperature, most plant physiological processes are disrupted (Ceglar *et al.* 2019), and damage may occur to fruit trees and agricultural crops (FAO 2024). The changes in SGS and LSF dates were assessed for each grid cell by comparing the base (1995–2014) with the 2041–2060 and 2081–2100 periods. The statistical significance of the observed changes was evaluated using the Student’s *t*-test. Changes were considered statistically significant if  $p < 0.05$ .

### Definition of false spring events

The FS event was identified in a given grid cell if the LSF occurred after the SGS. Changes in the future frequency and spatial distribution of these compound events were assessed. FS event intensity was also evaluated using accumulated GDD before the event (Eq. 1):

$$\text{GDD} = t_{avg} - t_{base} \quad (1),$$

where  $t_{avg}$  is the daily average air temperature, and  $t_{base}$  is the threshold temperature. If on a given day  $t_{avg} < t_{base}$ , then  $t_{avg}$  is set equal to  $t_{base}$  (McMaster, Wilhelm 1997).

Depending on the plant species,  $t_{base}$  may vary (Anandhi 2016; Kukal, Irmak 2018; Giolo *et al.* 2021). However, this study used  $t_{base} = 5^{\circ}\text{C}$  as this threshold is most suitable for crops in cooler and mid-latitude climates, especially cereals (Ruosteenoja *et al.* 2016). Moreover, the same  $5^{\circ}\text{C}$  threshold was used to determine the SGS.

To assess FS event intensity, these compound climatic events were categorised into three intensity categories based on the GDD accumulated before the event:

- **GDD1:**  $0^{\circ}\text{C} < \text{GDD} \leq 100^{\circ}\text{C}$ ;
- **GDD2:**  $100^{\circ}\text{C} < \text{GDD} \leq 200^{\circ}\text{C}$ ;
- **GDD3:**  $\text{GDD} > 200^{\circ}\text{C}$ .

The higher the intensity category, the more severe the event. The study assessed how the accumulated GDD before FS events and the share of events in each intensity category will change by the mid- and late-21st century.

## RESULTS

### SGS, LSF dates, and FS events in 1995–2014

Using ERA5 data, the dates of SGS and LSF, as well as FS events and their spatial distribution were assessed during the baseline period of 1995–2014. The 12th of April was the median SGS date over the two decades in the study area. A latitudinal pattern is apparent in the spatial distribution of the median SGS date. The earliest median SGS date was recorded in the south-western and southern parts of the study area (30 March), while the latest occurred in the northern part (24 April) (Fig. 2a).

During 1995–2014, the LSF date occurred nearly two weeks later than the SGS date, with a median of 25 April. A spatial pattern is also evident in the median LSF date, with the northern part of the study area showing LSF occurring 10–15 days later than in the south. However, the distance from the Baltic Sea was the primary factor influencing the spatial variation in LSF date. Grid cells located along the coast in western Lithuania had the earliest LSF dates, with a median date of 4 April. In contrast, the latest LSF date was observed in central Estonia (5–6 May) (Fig. 2b).

The distance from the Baltic Sea was also the main factor determining the spatial distribution of FS events during 1995–2014. Due to LSF occurring early in coastal regions, these areas recorded the fewest FS events – only 1–2 per decade, with none recorded in some grid cells. As the distance from the Baltic

Sea increased, so did the frequency of FS events. The highest number of these compound climate events (9.5 per decade) occurred in the eastern and south-eastern parts of the study area (Fig. 2c).

The GDD sum accumulated until the FS event was also assessed (Fig. 2d). The median value of this variable in the study area was approximately 58.5 °C. The highest GDD sums were observed in the southern part

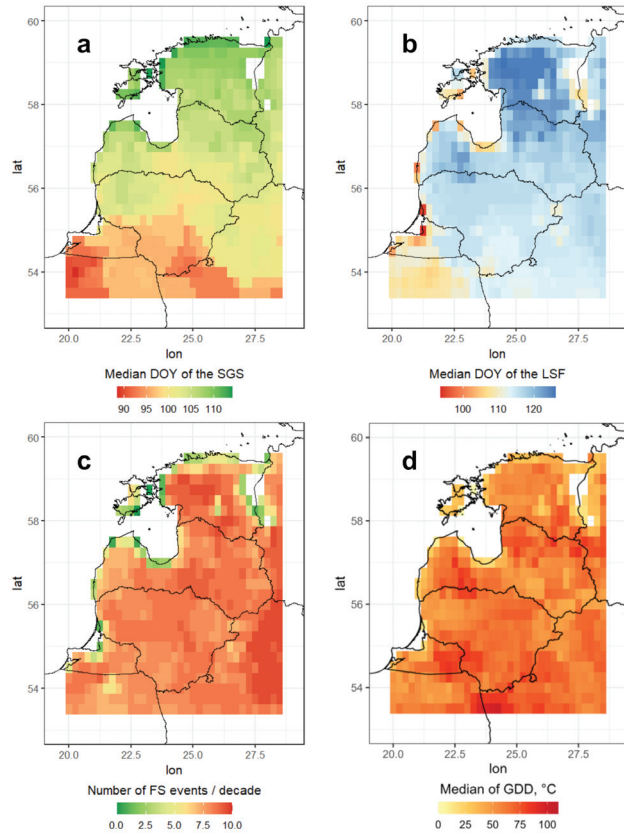


**Fig. 2** Median SGS date (DOY) (a), median LSF date (DOY) (b), number of FS events per decade (c), and median GDD sums (°C), accumulated until FS events (d) during 1995–2014

of the study area (95–102 °C), whereas coastal areas showed the lowest values for this variable, indicating weaker FS event intensity (Fig. 2d).

### Future projections of SGS and LSF dates

Using data from five different CMIP6 models under the SSP2-4.5 and SSP5-8.5 scenarios, a significant shift of SGS toward earlier dates was identified for the periods 2041–2060 and 2081–2100, compared to the baseline period of 1995–2014.

By 2041–2060, the SGS is projected to advance by 5–14.5 days under SSP2-4.5 and by 3–17.5 days under SSP5-8.5 (Fig. 3a). This advancement is evident across more than 90% of the study area. Except for the NorESM2-MM model, the SSP5-8.5 scenario consistently shows a 2–6 days earlier SGS compared to SSP2-4.5.

By the end of the 21<sup>st</sup> century, SGS dates are expected to shift even earlier. Under SSP2-4.5, SGS is projected to occur 9.5–27 days earlier, and under SSP5-8.5, 21–43 days earlier than during 1995–2014 (Fig. 3b). All models and both scenarios show statistically significant SGS advances across the entire territory, except for MPI-ESM1-2-LR and NorESM2-MM projections under the SSP2-4.5 scenario. The most prominent changes are projected using the CanESM5 and GFDL-CM4 models, which are characterised by high ECS values.

Similar trends were found for the LSF dates (Fig. 4). In 2041–2060, LSF is expected to occur 8–22 days earlier under SSP2-4.5 and 5.5–26.5 days earlier under SSP5-8.5, depending on the model (Fig. 4a). However, the scenario-driven differences are less consistent: only three models (CanESM5, GFDL-CM4, and MPI-ESM1-2-LR) project greater changes under SSP5-8.5 than under SSP2-4.5.

By 2081–2100, LSF is projected to shift 7–38 days

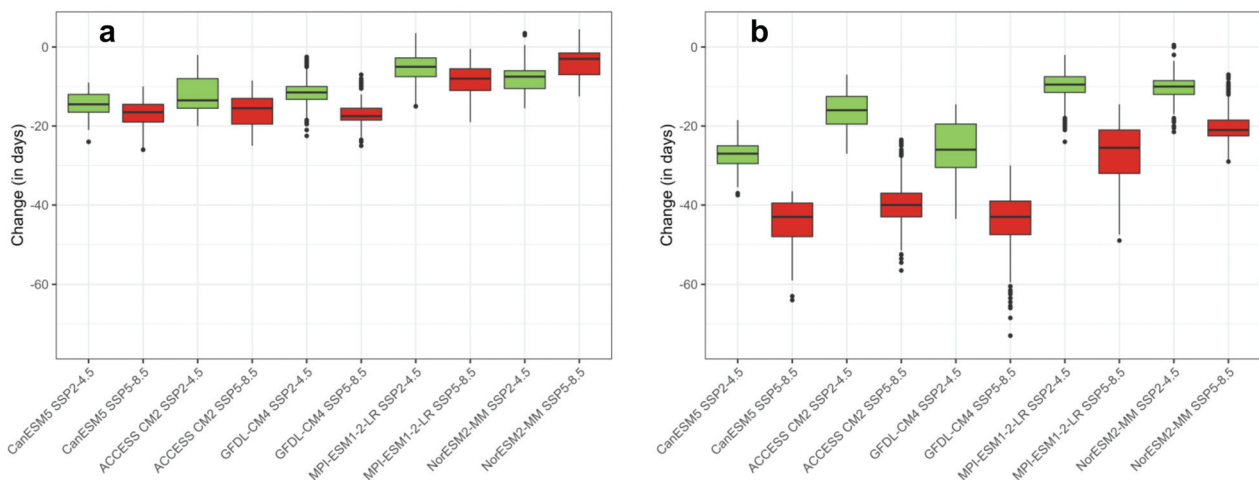


**Fig. 3** Box plots of SGS date changes (in days), comparing 2041–2060 (a) vs 1995–2014 and 2081–2100 vs 1995–2014 (b) based on five different CMIP6 models under two SSP scenarios. Green indicates the SSP2-4.5 scenario, and red represents SSP5-8.5

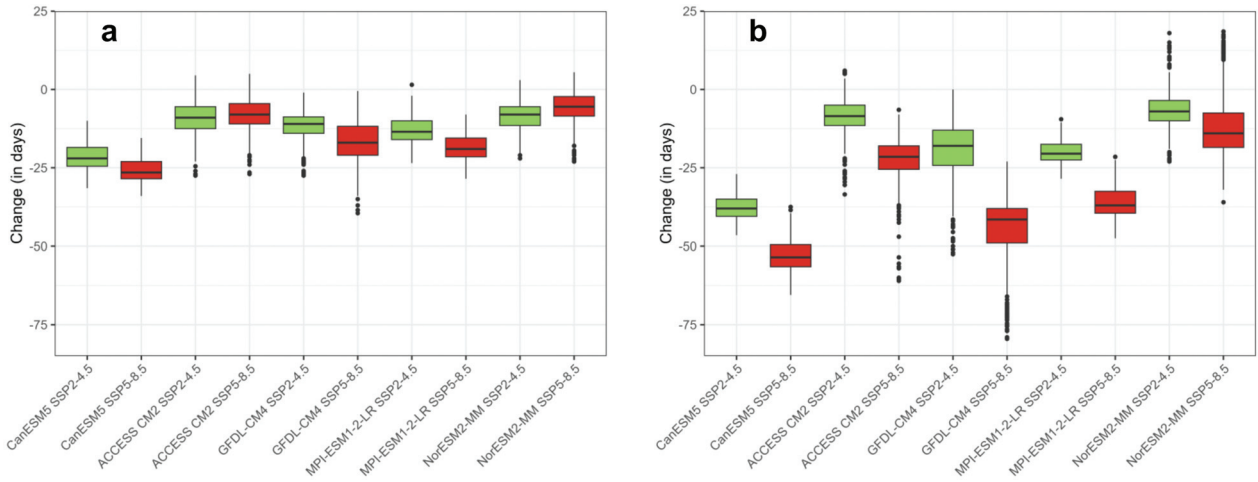


**Fig. 4** Box plots of LSF date changes (in days), comparing 2041–2060 (a) vs 1995–2014 and 2081–2100 vs 1995–2014 (b) based on five different CMIP6 models under two SSP scenarios. Green indicates the SSP2-4.5 scenario, and red represents SSP5-8.5

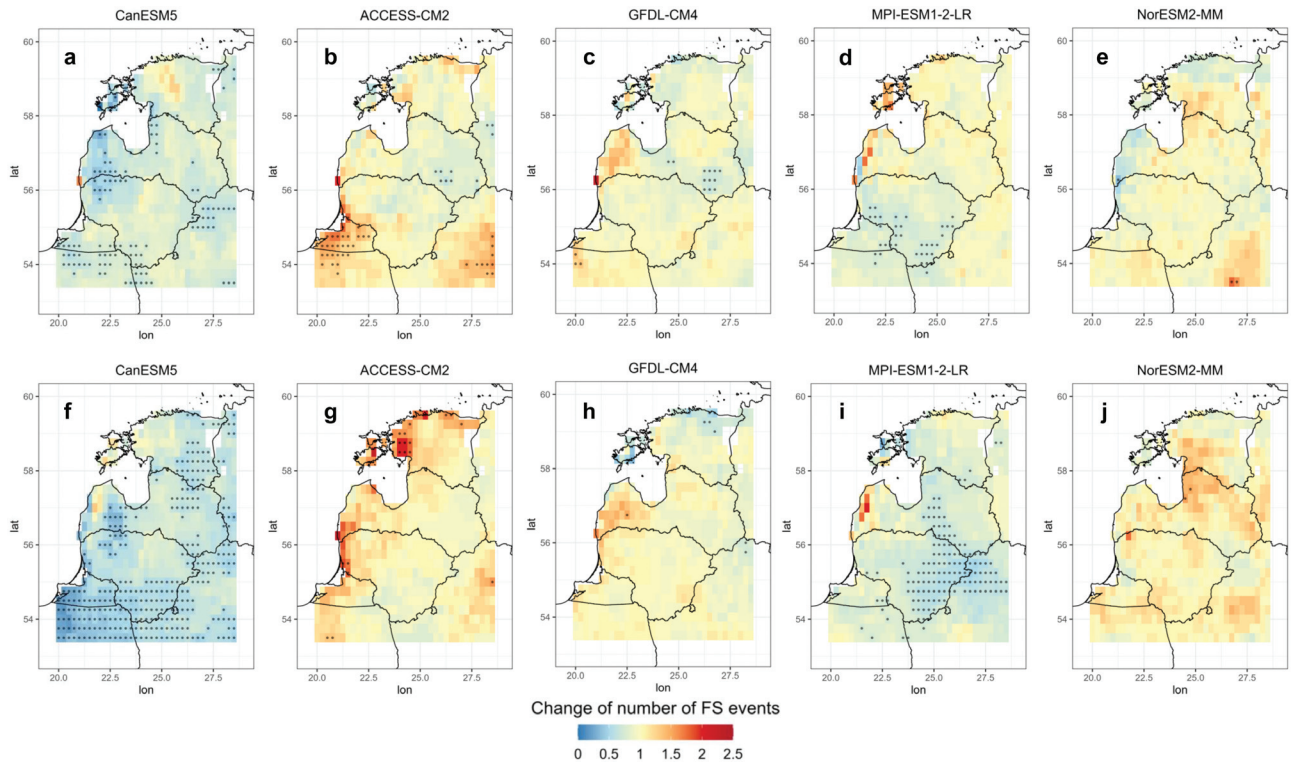


**Fig. 5** Changes in FS event frequency (number of occurrences) comparing the periods 2041–2060 vs 1995–2014 (a–e) and 2081–2100 vs 1995–2014 (f–j), based on SSP2-4.5 scenario data from different CMIP6 models. Dots indicate grid cells with statistically significant changes according to the Student's *t*-test (when  $p < 0.05$ )

earlier under SSP2-4.5 and 14–53.5 days earlier under SSP5-8.5. Although the trend of earlier LSF persists, for some models (ACCESS-CM2 under SSP2-4.5 and NorESM2-MM under both scenarios), the change affects a smaller portion of the area compared to mid-century (Fig. 4b). Nevertheless, all models show greater average LSF shifts under SSP5-8.5 than under SSP2-4.5. The most significant and widespread shifts – statistically significant ( $p < 0.05$ ) across the entire study area – are projected by CanESM5 under both scenarios and periods.

### Future projections of false spring events

Unlike the projections for SGS and LSF dates, future changes in the recurrence of FS events show no consistent pattern and are more uncertain. Under the SSP2-4.5 scenario for 2041–2060, most models project a decrease in FS events across much of the study area, with the most significant decline (96.4%) expected using CanESM5 model data (Fig. 5a).

By 2081–2100, an apparent decrease under SSP2-4.5 is projected only by three models (CanESM5,



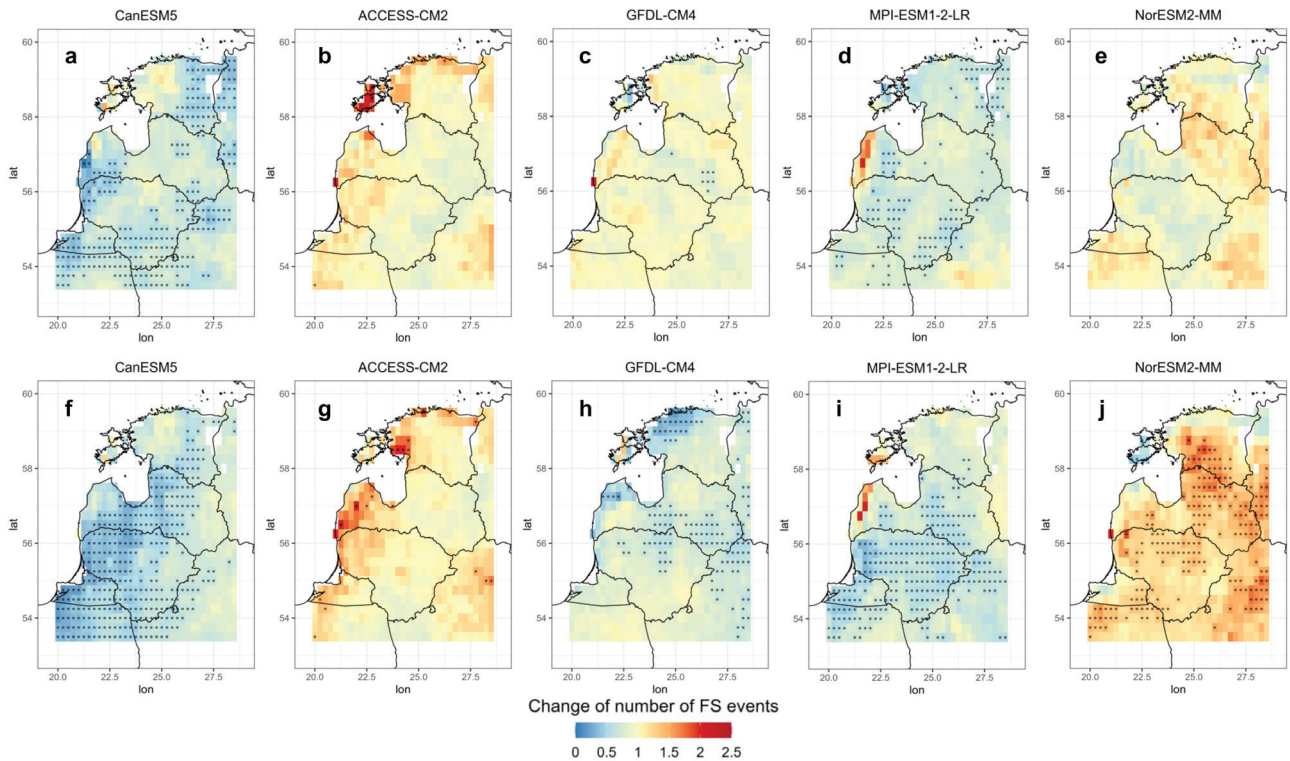


**Fig. 6** Same as Figure 5, but for the SSP5-8.5 scenario

GFDL-CM4, and MPI-ESM1-2-LR), while ACCESS-CM2 and NorESM2-MM show an increase of over 55% of the area (Fig. 5f–j). In most cases, changes under SSP2-4.5 are small, with statistically significant results in more than 10% of the study area only for CanESM5 and MPI-ESM1-2-LR.

Under SSP5-8.5, similar patterns emerge. For the period between 2041 and 2060, most models (except NorESM2-MM) project a decline in FS events, although only CanESM5 and MPI-ESM1-2-LR exhibit statistically significant decreases in over 20% of the area (Fig. 6a–e). However, for 2081–2100, three models (CanESM5, GFDL-CM4, and MPI-ESM1-2-LR) show a broad decline (over 94% of the area), while the other two (ACCESS-CM2 and NorESM2-MM) project increases in over half of the territory (Fig. 6f–j). The most significant and widespread changes, including statistically significant ones (up to 52.3% of grid cells), are again projected by CanESM5 (Fig. 6f).

In both periods and scenarios, the most significant increases and decreases are projected along the Baltic Sea coast, while the inland regions in the eastern part of the study area show minor, mostly non-significant changes. Overall, the most pronounced deviations from the 1995–2014 baseline are projected for 2081–2100 under SSP5-8.5 (Fig. 6f–j).

### Intensity of false spring events

Changes in the difference between LSF and SGS dates were analysed to assess whether future climate

conditions will favour the formation and increase in the intensity of FS events. Under the SSP2-4.5 scenario, projections for 2041–2060 suggest a decreasing difference between these dates in over half of the study area across all five CMIP6 models, with the highest mean reduction (4.2 days) forecasted by the MPI-ESM1-2-LR model (Table 2). However, by 2081–2100, the agreement between models is projected to weaken. CanESM5 and MPI-ESM1-2-LR project a further decrease (up to 12.6 days on average), while ACCESS-CM2 and GFDL-CM4 suggest a growing difference between LSF and SGS dates, indicating more favourable conditions for FS development.

Similar inconsistencies appear under the SSP5-8.5 scenario. By mid-century, four models (except ACCESS-CM2) predict a narrowing LSF–SGS gap, whereas by the century's end, ACCESS-CM2 and NorESM2-MM project an increase in the difference between these dates, with the most significant change expected (by 17.3 days on average) using the ACCESS-CM2 model's data.

Changes in the GDD accumulated before FS events align well with the observed patterns in changes of LSF–SGS: a smaller difference between these two dates corresponds to lower GDD. For 2041–2060, most models project reduced GDD sums, particularly under CanESM5 and MPI-ESM1-2-LR (down by, on average, 25.6–42.5 °C depending on the scenario). By 2081–2100, the reduction in the mean GDD sum accumulated until FS events is even higher in these models, while ACCESS-CM2 and NorESM2-MM predict increases up to 37.1 °C.

**Table 2** Percentage of the study area where, based on five different CMIP6 models and two SSP scenarios (SSP2-4.5 and SSP5-8.5), the difference between LSF and SGS dates is projected to decrease, increase, or remain unchanged in the periods 2041–2060 and 2081–2100 compared to the baseline period 1995–2014, along with the mean change in this difference (in days), and the change in mean GDD sums (°C) accumulated before FS events

Model	Period	SSP2-4.5 scenario					SSP5-8.5 scenario				
		Decrease, %	Increase, %	No change, %	Mean change of LSF–SGS, days	Mean change of GDD, °C	Decrease, %	Increase, %	No change, %	Mean change of LSF–SGS, days	Mean change of GDD, °C
CanESM5	2041–2060	78.4	16.2	5.5	–4.9	–25.6	97.6	1.5	1.0	–12.9	–42.5
	2081–2100	93.4	4.9	1.8	–12.6	–30.7	88.8	10.8	0.6	–10.1	–31.4
ACCESS-CM2	2041–2060	57.0	39.0	4.0	–0.9	–14.9	17.1	81.3	1.6	4.3	5.0
	2081–2100	10.5	87.9	1.6	6.5	14.6	2.5	97.5	0.0	17.3	35.3
GFDL-CM4	2041–2060	53.8	43.2	3.0	–0.9	–8.8	56.2	40.9	2.8	–1.8	–31.2
	2081–2100	23.5	75.1	1.3	6.1	1.6	72.4	25.5	2.1	–5.1	–30.5
MPI-ESM1-2-LR	2041–2060	70.0	23.7	6.4	–4.2	–27.9	91.3	6.0	2.8	–8.9	–36.8
	2081–2100	88.5	8.1	3.6	–9.2	–32.1	91.3	7.6	1.2	–10.8	–36.9
NorESM2-MM	2041–2060	56.7	39.4	3.9	–2.0	–21.4	61.8	34.3	3.9	–2.2	0.9
	2081–2100	49.8	47.7	2.5	0.4	3.8	31.9	64.5	3.6	5.1	37.1

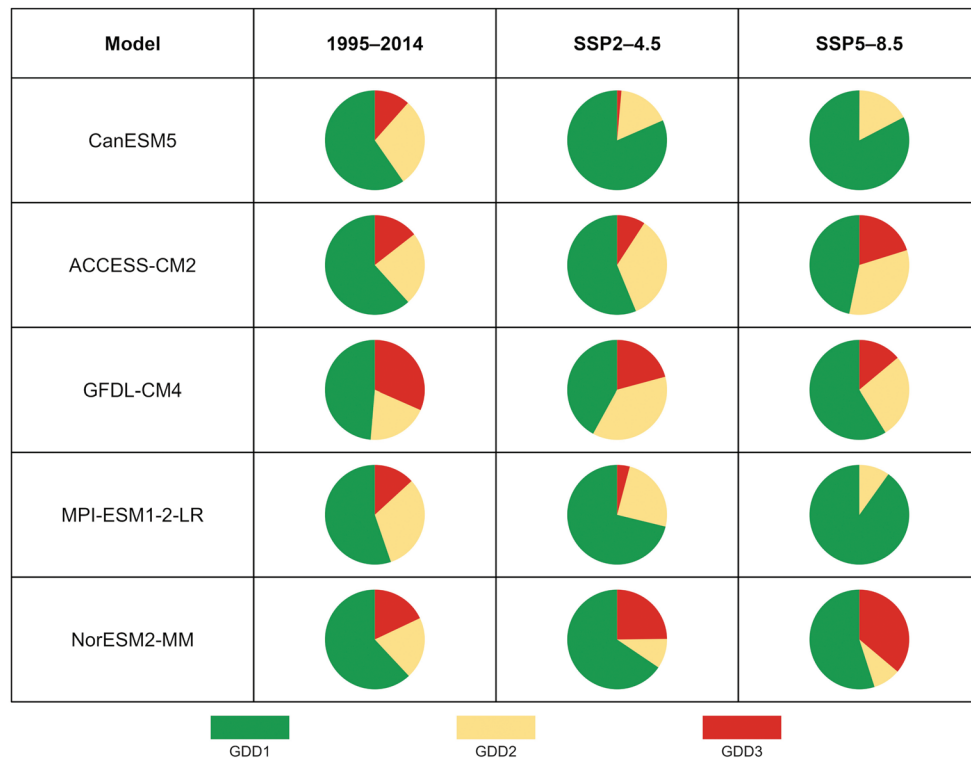


**Fig. 7** Percentage of FS events belonging to different intensity categories (%), based on data from five CMIP6 models for 1995–2014 and 2081–2100. Projections for 2081–2100 are based on SSP2-4.5 and SSP5-8.5 scenarios. More details on intensity categories are provided in Section 2.4

Lastly, projections of FS events belonging to different intensity categories for the period 2081–2100 also vary (Fig. 7). According to data from the CanESM5 and MPI-ESM1-2-LR models, fewer FS events are expected to fall into the highest intensity category (GDD3), with none anticipated under SSP5-8.5. In contrast, ACCESS-CM2 and NorESM2-MM foresee an increase in high-intensity events, especially under SSP5-8.5, where over one-third of FS events fall into the GDD3 category. Models projecting more FS events also anticipate greater intensity,

while those projecting fewer events indicate a decline in the severity of these events.

## DISCUSSION

During this research, a clear trend of SGS date advancement was identified across the entire study area for the mid- and late-21st century. Such a trend was observed in almost all grid cells, regardless of climate model and SSP scenario. It was also found that the changes are statistically significant in most



cases, with the most pronounced advancement of the SGS date projected for 2081–2100 under the SSP5-8.5 scenario. According to data from various climate models, by the end of the 21<sup>st</sup> century, the SGS date is expected to shift, on average, 3 to 6 weeks earlier than during the base period of 1995–2014. Similar trends of SGS date advancement are also projected in various regions of the Northern Hemisphere (Xia *et al.* 2015; Zhu *et al.* 2019). Ruosteenoja *et al.* (2016) found that under a pessimistic scenario, the SGS date in Europe could become 1 to 1.5 months earlier. An average advancement of 1.5 to 3.5 weeks by the end of the 21<sup>st</sup> century is also projected in Poland (Marcinkowski *et al.* 2023; Szyga-Pluta *et al.* 2023), while in Estonia, the growing season is expected to begin 1 to 1.5 months earlier by 2100 than in 1990 (Saue *et al.* 2015). Such SGS changes in the future are linked to the projected rise in the average air temperature. Therefore, the derived SGS date and its changes only reflect how the “window of opportunity” for the potential start of the growing season is expected to shift (Körner *et al.* 2023).

Similar to the changes in the SGS date, the LSF date will also shift earlier in the future, and this tendency is expected in the majority of grid cells. Depending on the model and scenario, by the middle of the 21<sup>st</sup> century these changes are expected to range from five days to nearly four weeks. By the end of the 21<sup>st</sup> century, the advancement of the LSF date is even greater. Compared to the 1995–2014 period, the LSF date is expected to shift earlier from one to six weeks on average. Similar to changes in the SGS date, the rise in  $t_{min}$  values resulting from anthropogenic climate change is the primary reason for the advancement of the LSF date. A shift in the LSF date to earlier has also been projected for other regions of the Northern Hemisphere, both in the near future and by the end of the 21<sup>st</sup> century (Charalampopoulos, Droulia 2022; Helali *et al.* 2022; Chen *et al.* 2024; Ford *et al.* 2025).

During the assessment of changes in SGS and LSF dates, it was observed that the CanESM5 model projects the most pronounced advancement of these dates. In contrast, the modest changes occurred while using the NorESM2-MM model's data. Depending on the period and SSP scenario, the CanESM5 model projects changes 7–22 days greater than those of the NorESM2-MM model. For LSF dates, this difference is even more pronounced, ranging from 14 to 39.5 days. This variability is primarily attributed to differences in ECS values among the models, with CanESM5 exhibiting the highest ECS values, and NorESM2-MM the lowest of the models assessed in this study (Table 1).

Although an overall shift to earlier dates is expected, individual models show different magnitudes of change in SGS and LSF. Some models project a larger

advancement in SGS compared to LSF, while others show a greater shift in LSF. These differences are reflected in the projected changes between the LSF and SGS dates. For the period between 2041 and 2060, all models project a reduction in this difference under the SSP2-4.5 scenario. Under the SSP5-8.5 scenario, a similar trend is projected by four out of five models used in this study. By the end of the century, a decrease in the mean difference between LSF and SGS dates is projected by two models under SSP2-4.5 and by three models under SSP5-8.5. In these cases, the LSF date is expected to advance more than the SGS date, implying less favourable conditions for the formation of FS events. However, the remaining models suggest an increase in the difference between LSF and SGS dates, indicating a more rapid advancement of the SGS date compared to the LSF date.

The different rates of change in LSF and SGS dates have been predicted to result in projected changes in the recurrence of FS events showing no consistent pattern, unlike those in SGS or LSF dates. It has been observed that according to model scenarios that predict a decrease in the difference between LSF and SGS dates, the number of FS events will also be lower in most cases in the future, and *vice versa*. Therefore, in this case, the ECS values of the models, unlike when assessing changes in SGS and LSF dates, are not so essential in determining the magnitude of future changes. If a more rapid temperature increase is projected for the end of winter or early spring, the number of FS events may rise; however, if more significant warming is expected in the second half of spring, the number of FS events may decrease.

For the period between 2041 and 2060, most models indicate a decreasing trend in the number of FS events. Meanwhile, by the end of the 21<sup>st</sup> century, these compound climate events are projected to increase according to two models and decrease according to the remaining three. However, in most cases, the projected changes are not substantial. Similar FS event projections have also been observed in other regions, which are characterised by high uncertainty and the absence of a unified trend. In some areas, an increase in the number of these events is expected, while in others a decrease is projected (Allstadt *et al.* 2015; Martinuzzi *et al.* 2019; Lhotka, Brönnimann 2020; Masaki 2020; Mallard *et al.* 2023). Therefore, forecasting future changes in FS events remains a complex task (Allstadt *et al.* 2015).

The mean changes in the difference between LSF and SGS dates are consistent with changes in the mean sums of GDD accumulated before FS events. It was found that as the difference between LSF and SGS decreases, the amount of GDD accumulated before an FS event also declines. The intensity of FS events was also assessed by classifying these events

into three intensity categories based on the sum of GDD accumulated until the event. The tendency was observed where models predicting an increase in the number of FS events also forecast an increase in the intensity of these compound climate events. An increasing intensity of FS events is also projected for France (Vautard *et al.* 2023), certain regions of China (Chen *et al.* 2024), and south-eastern Europe (Charalampopoulos, Droulia 2022). However, according to the remaining models used in this study, which project a decrease in FS events, the intensity of these compound climate events is expected to diminish.

In this study, FS events were assessed using a meteorological approach – this approach was employed to determine the SGS date and to evaluate the intensity of FS events. However, the risk and potential damage of FS events also depend on other factors, primarily the plant species, precipitation levels, soil moisture, local topography, and other variables (Chamberlain *et al.* 2019; Ma *et al.* 2019). Therefore, to improve the prediction of these compound climate events, future studies should consider the influence of these variables.

Furthermore, the intensity of FS events was evaluated based on the sum of GDD accumulated prior to an FS event. By doing this, a widely accepted assumption was applied, whereby a higher accumulation of GDD corresponds to greater potential damage caused by an FS event. This assumption is appropriate, as it has been proven that the accumulated GDD sum determines the plant developmental stage, and the later in spring the FS event occurs, the more severe the damage it causes (Miller *et al.* 2001; Chun, Changnon 2018; Qiu *et al.* 2024; Bhatti *et al.* 2025). However, the GDD method has limitations. In this study,  $t_{\text{base}} = 5\text{ }^{\circ}\text{C}$  was applied for the calculation of GDD; however, to assess the impact of FS events on specific plant species more accurately, different  $t_{\text{base}}$  values should be considered (Chamberlain, Walkovich 2023). Finally, plant development depends not only on temperature and GDD but also on moisture availability. When moisture levels are low, even if the required GDD sum has been reached, the particular phenological stage may not be reached and, as a result, the damage caused by an FS event may vary accordingly (Miller *et al.* 2001).

Another limitation encountered in this study is the spatial resolution of grid cells ( $\sim 25\text{ km}$ ), which may be too coarse to evaluate local-scale changes. Finally, the NEX-GDDP-CMIP6 dataset used in this study also has some limitations. The BCSDB bias correction method used to produce this dataset is based on the assumption that the spatial climate patterns observed between 1960 and 2014 will persist unchanged in the future. It also retains the original trend slopes of GCM projections, thereby maintaining the rate of

change defined by the original scenario. Although the method includes bias correction and offers finer spatial resolution, it only applies linear adjustments to projection offsets, which may not adequately reflect the nonlinear dynamics of climate systems (Thrasher *et al.* 2012). Furthermore, since a constant bias across different distribution quantiles is assumed, future extremes may remain inadequately assessed (Zhang *et al.* 2024).

## CONCLUSIONS

During this study, future projections of FS events recurrence and intensity in the eastern part of the Baltic Sea region were developed using the data from five different CMIP6 models and two SSP scenarios (SSP2-4.5 and SSP5-8.5). These projections were generated for 2041–2060 and 2081–2100. Changes in SGS and LSF dates were also evaluated.

According to all five climate models and two SSP scenarios, the SGS date is projected to advance in the future compared to the 1995–2014 reference period. During 2041–2060, the SGS date, depending on the model, is expected to shift earlier by 5–14.5 days under the SSP2-4.5 scenario and by 3–17.5 days under the SSP5-8.5 scenario. By 2081–2100, this change is projected to reach 9.5–27 days and 21–43 days, respectively. A similar trend is also projected for the LSF date across all models used. In the mid-21st century, the LSF date is expected to occur 8–22 days earlier under SSP2-4.5 and 5.5–26.5 days earlier under the SSP5-8.5 scenario. By the end of the 21<sup>st</sup> century, these changes are projected to increase to 7–38 days and 14–53.5 days, respectively. The most significant changes in SGS and LSF dates are projected using the CanESM5 scenario data, which is characterised by the highest ECS value.

Both LSF and SGS dates are projected to shift earlier; however, the magnitude of these changes will vary depending on the climate model used. This variability results in the absence of a clear tendency in the projections of future FS events. For the period between 2041 and 2060, most models predict a general decline in the frequency of these compound climate events. However, for the period between 2081 and 2100, only three models continue to project a decreasing trend, while the remaining two predict an increase in the number of FS events. During the assessment of FS event intensity, it was observed that models and scenarios projecting a decline in FS event frequency also indicate a decrease in their intensity – and *vice versa*.

This study focused on future FS event projections in the eastern part of the Baltic Sea region for the first time. As such, it may serve as a foundational step toward more detailed and accurate forecasts and

the evaluation of risks posed by these events to fruit trees, crops, and other sectors. These insights could help create adaptation strategies to reduce the potential damage of FS events in a changing climate.

## ACKNOWLEDGMENTS

We thank two anonymous reviewers for their insightful advice and constructive comments.

## REFERENCES

- Allstadt, A.J., Vavrus, S.J., Heglund, P.J., Pidgeon, A.M., Thogmartin, W.E., Radeloff, V.C. 2015. Spring plant phenology and false springs in the conterminous US during the 21st century. *Environmental Research Letters* 10(10). <https://doi.org/10.1088/1748-9326/10/10/104008>
- Anandhi, A. 2016. Growing degree days – Ecosystem indicator for changing diurnal temperatures and their impact on corn growth stages in Kansas. *Ecological Indicators* 61, 149–158. <https://doi.org/10.1016/j.ecolind.2015.08.023>
- Augsburger, C.K. 2013. Reconstructing patterns of temperature, phenology, and frost damage over 124 years: Spring damage risk is increasing. *Ecology* 94(1), 41–50. <https://doi.org/10.1890/12-0200.1>
- Ault, T.R., Henebry, G.M., DeBeurs, K.M., Schwartz, M.D., Betancourt, J.L., Moore, D. 2013. The false spring of 2012, earliest in North American record. *Eos* 94(20), 181–182. <https://doi.org/10.1002/2013EO200001>
- Ball, M.C., Harris-Pascal, D., Egerton, J.J.G., Lenné, T. 2011. The paradoxical increase in freezing injury in a warming climate: Frost as a driver of change in cold climate vegetation. *Temperature Adaptation in a Changing Climate: Nature at Risk November 2011*, 179–185. <https://doi.org/10.1079/9781845938222.0179>
- Bateman, B. 2022. *False Springs: How Earlier Spring With Climate Change Wreaks Havoc on Birds*. [online] Audubon. Available at: <https://www.audubon.org/news/false-springs-how-earlier-spring-climate-change-wreaks-havoc-birds> [Accessed 28 April 2025].
- Baumgarten, F., Gessler, A., Vitasse, Y. 2023. No risk – no fun: Penalty and recovery from spring frost damage in deciduous temperate trees. *Functional Ecology* 37(3), 648–663. <https://doi.org/10.1111/1365-2435.14243>
- Beck, H.E., Zimmermann, N.E., McVicar, T.R., Vergopolan, N., Berg, A., Wood, E.F. 2018. Present and future Köppen-Geiger climate classification maps at 1-km resolution. *Scientific data* 5(1), 1–12. <https://doi.org/10.1038/sdata.2018.214>
- Bhatti, S., Jeranyama, P., Kennedy, C.D., Buda, A.R., Ghantous, K., Millar, D.J., DeMoranville, C.J. 2025. Changes in cranberry phenology from 1958 to 2022: Implications for spring frost protection in Massachusetts, United States. *International Journal of Biometeorology* 69, 1297–1309. <https://doi.org/10.1007/s00484-025-02892-w>
- Bosdijk, J., de Feiter, V.S., Gaiser, A., Smink, T., Thorkeldsdottir, G., van Vliet, A.J.H., Luedeling, E. 2024. False springs in the Netherlands: climate change impact assessment with the false spring damage indicator model. *Regional Environmental Change* 24(2), 1–11. <https://doi.org/10.1007/s10113-024-02235-2>
- Cannell, M.G.R., Smith, R.I. 1986. Climatic Warming, Spring Budburst and Forest Damage on Trees. *Journal of Applied Ecology* 23(1), 177–191. <https://doi.org/10.2307/2403090>
- Carter, T.R. 1998. Changes in the thermal growing season in Nordic countries during the past century and prospects for the future. *Agricultural and Food Science in Finland* 7(2), 161–179. <https://doi.org/10.23986/afsci.72857>
- Ceglar, A., Zampieri, M., Toreti, A., Dentener, F. 2019. Observed northward migration of agro-climate zones in Europe will further accelerate under climate change. *Earth's Future* 7(9), 1088–1101. <https://doi.org/10.1029/2019EF001178>
- Chamberlain, C.J., Wolkovich, E.M. 2023. Variation across space, species and methods in models of spring phenology. *Climate Change Ecology* 5, 100071. <https://doi.org/10.1016/j.ecochg.2023.100071>
- Chamberlain, C.J., Cook, B.I., García de Cortázar-Atauri, I., Wolkovich, E.M. 2019. Rethinking false spring risk. *Global Change Biology* 25(7), 2209–2220. <https://doi.org/10.1111/gcb.14642>
- Chamberlain, C.J., Cook, B.I., Morales-Castilla, I., Wolkovich, E.M. 2021. Climate change reshapes the drivers of false spring risk across European trees. *New Phytologist* 229(1), 323–334. <https://doi.org/10.1111/nph.16851>
- Charalampopoulos, I., Droulia, F. 2022. Frost Conditions Due to Climate Change in South-Eastern Europe via a High-Spatio temporal-Resolution Dataset. *Atmosphere* 13(9), 1407. <https://doi.org/10.3390/atmos13091407>
- Chen, D., Rojas, M., Samset, B.H., Cobb, K., Diongue Niang, A., Edwards, P., Emori, S., Faria, S.H., Hawkins, E., Hope, P., Huybrechts, P., Meinshausen, M., Mustafa, S.K., Plattner, G.K., Tréguier, A.-M. 2021. *Framing, context, and methods*. In: V. Masson-Delmotte, P. Zhai, A. Pirani, S.L. Connors, C. Péan, S. Berger, N. Caud, Y. Chen, L. Goldfarb, M.I. Gomis, M., Huang, K., Leitzell, E., Lonnoy, J.B.R., Matthews, T.K., Maycock, T., Waterfield, O., Yelekçi, R. Yu, Zhou, B., eds. *Climate Change 2021: The Physical Science Basis. Contribution of Working Group I to the Sixth Assessment Report of the Intergovernmental Panel on Climate Change*. Cambridge: Cambridge University Press, 147–286 pp. <https://doi.org/10.1017/9781009157896.003>
- Chen, R., Wang, J., Li, Y., Bai, R., Huang, M., Zhang, Z., Zhao, L., Qu, Z., Liu, L. 2024. Higher risk of spring frost under future climate change across China's apple planting regions. *European Journal of Agronomy* 159 (May), 127288. <https://doi.org/10.1016/j.eja.2024.127288>
- Chun, S.E., Changnon, D. 2019. Predicting major peach yield reductions in the Midwest and Southeast United



- States. *Meteorological Applications* 26(1), 97–107. <https://doi.org/10.1002/met.1740>
- Clark, R.M., Thompson, R. 2010. Predicting the impact of global warming on the timing of spring flowering. *International Journal of Climatology* 30(11), 1599–1613. <https://doi.org/10.1002/joc.2004>
- Cook, B.I., Chamberlain, C., Wolkovich, E.M., Morales-Castilla, I. 2020. *Climate change reshapes the drivers of false spring risk across European trees*. [online] Nasa. gov. Available at: <https://ntrs.nasa.gov/citations/20205006353> [Accessed 30 April 2025].
- Crassweller, R. 2024. *Frost, Critical Temperatures, and Frost Protection*. [online] Available at: <https://extension.psu.edu/frost-critical-temperatures-and-frost-protection> [Accessed 29 April 2025].
- ECMWF. 2021. *CMIP6 climate projections*. Copernicus. eu. <https://doi.org/10.24381/cds.c866074c>
- European Climate Risk Assessment. 2024. *European Environment Agency*, Luxembourg: Publications Office of the European Union, 486 pp. <https://doi.org/10.2800/8671471>
- FAO. 2024. *Frost protection: fundamentals, practice, and economics – Volume 1*. [online] Available at: <https://www.fao.org/4/y7223e/y7223e0a.htm>. [Accessed 30 April 2025].
- Faust, E., Herbold, J. 2017. Spring frost losses and climate change – Not a contradiction in terms. *Topics Geo May*, 1–11.
- Ford, T.W., Chen, L., Fernandez, E., Wahle, E., Luedeling, E., Todey, D., Nowatzkie, L., Agronomía, E.De, Cat, P.U. 2025. Agricultural and Forest Meteorology Historical and Projected Changes in Chill Accumulation and Spring Freeze Risk in the Midwest United States. *Agricultural and Forest Meteorology* 368 (March), 110532. <https://doi.org/10.1016/j.agrformet.2025.110532>
- Giolo, M., Sallenave, R., Pornaro, C., Velasco-Cruz, C., Macolino, S., Leinauer, B. 2021. Base temperatures affect accuracy of growing degree day model to predict emergence of bermuda grasses. *Agronomy Journal* 113(3), 2960–2966. <https://doi.org/10.1002/agj2.20660>
- Graczyk, D., Szwed, M. 2020. Changes in the occurrence of late spring frost in Poland. *Agronomy* 10(11). <https://doi.org/10.3390/agronomy10111835>
- Grigorieva, E., Livenets, A., Stelmakh, E. 2023. Adaptation of Agriculture to Climate Change: A Scoping Review. *Climate* 11(10), 1–37. <https://doi.org/10.3390/cli11100202>
- Grossman, E. 2014. *Why You Shouldn't Hope for An Early Spring*. [online] *Climate Central*. Available at: <https://www.climatecentral.org/news/why-you-shouldnt-hope-for-an-early-spring-17105> [Accessed 29 April 2025].
- Hájková, L., Možný, M., Oušková, V., Bartošová, L., Dížková, P., Žalud, Z. 2023. Increasing Risk of Spring Frost Occurrence during the Cherry Tree Flowering in Times of Climate Change. *Water (Switzerland)* 15(3). <https://doi.org/10.3390/w15030497>
- Hausfather, Z. 2018. *Explainer: How scientists estimate climate sensitivity*. [online] *Carbon Brief*. Available at: <https://www.carbonbrief.org/explainer-how-scientists-estimate-climate-sensitivity/> [Accessed 30 April 2025].
- Hausfather, Z. 2019. *CMIP6: the next generation of climate models explained – Carbon Brief*. [online] *Carbon Brief*. Available at: <https://www.carbonbrief.org/cmip6-the-next-generation-of-climate-models-explained/> [Accessed 30 April 2025].
- Helali, J., Oskouei, E.A., Hosseini, S.A., Saeidi, V., Modirian, R. 2022. Projection of changes in late spring frost based on CMIP6 models and SSP scenarios over cold regions of Iran. *Theoretical and Applied Climatology* 149(3–4), 1405–1418. <https://doi.org/10.1007/s00704-022-04124-2>
- Hersbach, H., Bell, B., Berrisford, P., Hirahara, S., Horányi, A., Muñoz-Sabater, J., Nicolas, J., Peubey, C., Radu, R., Schepers, D., Simmons, A., Soci, C., Abdalla, S., Abellan, X., Balsamo, G., Bechtold, P., Biavati, G., Bidlot, J., Bonavita, M., ... Thépaut, J.N. 2020. The ERA5 global reanalysis. *Quarterly Journal of the Royal Meteorological Society* 146(730), 1999–2049. <https://doi.org/10.1002/qj.3803>
- Hufkens, K., Friedl, M.A., Keenan, T.F., Sonnentag, O., Bailey, A., O'Keefe, J., Richardson, A.D. 2012. Ecological impacts of a widespread frost event following early spring leaf-out. *Global Change Biology* 18(7), 2365–2377. <https://doi.org/10.1111/j.1365-2486.2012.02712.x>
- Jarzyna, K. 2021. Climatic hazards for native tree species in Poland with special regards to silver fir (*Abies alba* Mill.) and European beech (*Fagus sylvatica* L.). *Theoretical and Applied Climatology* 144(1–2), 581–591. <https://doi.org/10.1007/s00704-021-03550-y>
- Jeong, S.J., Ho, C.H., Gim, H.J., Brown, M.E. 2011. Phenology shifts at start vs. end of growing season in temperate vegetation over the Northern Hemisphere for the period 1982–2008. *Global Change Biology* 17(7), 2385–2399. <https://doi.org/10.1111/j.1365-2486.2011.02397.x>
- Kilkus, K., Stonevičius, E. 2011. *Lietuvos vandenų geografija*. Lithuania: Vilniaus universitetas, 188 pp. [In Lithuanian].
- Klimavičius, L., Rimkus, E. 2024. False spring events in the eastern part of the Baltic Sea region. *Theoretical and Applied Climatology* 155, 9351–9365. <https://doi.org/10.1016/j.oceano.2023.06.010>
- Körner, C., Möhl, P., Hiltbrunner, E. 2023. Four ways to define the growing season. *Ecology Letters* 26(8), 1277–1292. <https://doi.org/10.1111/ele.14260>
- Koźmiński, C., Mąkosza, A., Nidzgorska-Lencewicz, J., Michalska, B. 2023. Air Frosts in Poland in the Thermal Growing Season (AT > 5 °C). *Agriculture (Switzerland)* 13(6). <https://doi.org/10.3390/agriculture13061228>
- Kukal, M.S., Irmak, S. 2018. U.S. Agro-Climat in 20th Century: Growing Degree Days, First and Last Frost, Growing Season Length, and Impacts on Crop Yields. *Scientific Reports* 8(1), 1–14. <https://doi.org/10.1038/s41598-018-25212-2>

- Lhotka, O., Brönnimann, S. 2020. Possible increase of vegetation exposure to spring frost under climate change in Switzerland. *Atmosphere* 11(4). <https://doi.org/10.3390/ATMOS11040391>
- Liu, Q., Piao, S., Janssens, I.A., Fu, Y., Peng, S., Lian, X., Ciais, P., Myneni, R.B., Peñuelas, J., Wang, T. 2018. Extension of the growing season increases vegetation exposure to frost. *Nature Communications* 9(1). <https://doi.org/10.1038/s41467-017-02690-y>
- Liu, R., Zhang, X., Wang, W., Wang, Y., Liu, H., Ma, M., Tang, G. 2024. Global-scale ERA5 product precipitation and temperature evaluation. *Ecological Indicators* 166 (January), 112481. <https://doi.org/10.1016/j.ecolind.2024.112481>
- Ma, Q., Huang, J.G., Hänninen, H., Berninger, F. 2019. Divergent trends in the risk of spring frost damage to trees in Europe with recent warming. *Global Change Biology* 25(1), 351–360. <https://doi.org/10.1111/gcb.14479>
- Mallard, M.S., Talgo, K.D., Spero, T.L., Bowden, J.H., Nolte, C.G. 2023. Dynamically Down scaled Projections of Phenological Changes across the Contiguous United States. *Journal of Applied Meteorology and Climatology* 62(12), 1875–1889. <https://doi.org/10.1175/JAMC-D-23-0071.1>
- Marcinkowski, P., Piniewski, M., Jefimow, M. 2023. Assessment of projected climate change impact on agro-climatic indicators in Poland. *International Journal of Climatology* 43(13), 6003–6019. <https://doi.org/10.1002/joc.8185>
- Martinuzzi, S., Allstadt, A.J., Pidgeon, A.M., Flather, C.H., Jolly, W.M., Radeloff, V.C. 2019. Future changes in fire weather, spring droughts, and false springs across U.S. National Forests and Grasslands. *Ecological Applications* 29(5), 1–14. <https://doi.org/10.1002/eap.1904>
- Masaki, Y. 2020. Future risk of frost on apple trees in Japan. *Climatic Change* 159(3), 407–422. <https://doi.org/10.1007/s10584-019-02610-7>
- McMaster, G.S., Wilhelm, W.W. 1997. Growing degree-days: One equation, two interpretations. *Agricultural and Forest Meteorology* 87(4), 291–300. [https://doi.org/10.1016/S0168-1923\(97\)00027-0](https://doi.org/10.1016/S0168-1923(97)00027-0)
- McNicholl, B., Lee, Y.H., Campbell, A.G., Dev, S. 2022. Evaluating the Reliability of Air Temperature from ERA5 Reanalysis Data. *IEEE Geoscience and Remote Sensing Letters* 19, 1–5. <https://doi.org/10.1109/LGRS.2021.3137643>
- Miller, P., Lanier, W., Brandt, S. 2001. Using Growing Degree Days to Predict Plant Stages. Ag/Extension Communications Coordinator, Communications Services, Montana State University-Bozeman, Bozeman. *MO* 59717(406).
- Miš, F., Tomczyk, A.M. 2025. Spatial and temporal differentiation of the thermal growing season in central and northern Europe. *Theoretical and Applied Climatology* 156(2). <https://doi.org/10.1007/s00704-025-05382-6>
- Monahan, W.B., Rosemartin, A., Gerst, K.L., Fisichelli, N.A., Ault, T.R., Schwartz, M.D., Gross, J.E., Weltzin, J.F. 2016. Climate change is advancing spring onset across the U.S. national park system. *Ecosphere* 7(10), e01465. <https://doi.org/10.1002/ecs2.1465>
- Muffler, L., Weigel, R., Beil, I., Leuschner, C., Schmeddes, J., Kreyling, J. 2024. Winter and spring frost events delay leaf-out, hamper growth and increase mortality in European beech seedlings, with weaker effects of subsequent frosts. *Ecology and Evolution* 14(7), e70028. <https://doi.org/10.1002/ece3.70028>
- Nidzgorska-Lencewicz, J., Mąkosza, A., Koźmiński, C., Michalska, B. 2024. Potential risk of Frost in the growing season in Poland. *Agriculture* 14(3), 501. <https://doi.org/10.3390/agriculture14030501>
- Peltonen-Sainio, P., Jauhiainen, L., Hakala, K., Ojanen, H. 2009. Climate change and prolongation of growing season: Changes in regional potential for field crop production in Finland. *Agricultural and Food Science* 18(3–4), 171–190. <https://doi.org/10.2137/145960609790059479>
- Peterson, A.G., Abatzoglou, J.T. 2014. Observed changes in false springs over the contiguous United States. *Geophysical Research Letters* 41(6), 2156–2162. <https://doi.org/10.1002/2014GL059266>
- Piotrowski, P., Bartoszek, K. 2025. Atmospheric Circulation Conditions During Spring Frosts in South-eastern Poland (1981–2023). *Atmosphere* 16(4), 409. <https://doi.org/10.3390/atmos16040409>
- Qiu, H., Yan, Q., Yang, Y., Huang, X., Wang, J., Luo, J., Peng, L., Bai, G., Zhang, L., Zhang, R., Fu, Y.H., Wu, C., Peñuelas, J., Chen, L. 2024. Flowering in the Northern Hemisphere is delayed by frost after leaf-out. *Nature communications* 15(1), 9123. <https://doi.org/10.1038/s41467-024-53382-3>
- Rao, K.K., Al Mandous, A., Al Ebri, M., Al Hameli, N., Rakib, M., Al Kaabi, S. 2024. Future changes in the precipitation regime over the Arabian Peninsula with special emphasis on UAE: insights from NEX-GDDP CMIP6 model simulations. *Scientific Reports* 14(1), 1–21. <https://doi.org/10.1038/s41598-023-49910-8>
- Rodrigo, J. 2000. Spring frosts in deciduous fruit trees. Morphological damage and flower hardiness. *Scientia Horticulturae* 85(3), 155–173. [https://doi.org/10.1016/S0304-4238\(99\)00150-8](https://doi.org/10.1016/S0304-4238(99)00150-8)
- Ruosteenoja, K., Räisänen, J., Venäläinen, A., Kämäräinen, M. 2016. Projections for the duration and degree days of the thermal growing season in Europe derived from CMIP5 model output. *International Journal of Climatology* 36(8), 3039–3055. <https://doi.org/10.1002/joc.4535>
- Saue, T., Käremaa, K., Nejedlik, P., Eliášová, M. 2015. Lengthening of the thermal growing season due climate change in Estonia. In: Šiška et al. (eds) *Towards climatic services, Nitra*.
- SMHI. 2025. *Length of the vegetation period*. [online] Available at: <https://www.smhi.se/en/climate/tools-and-inspiration/climate-indicators/length-of-the-vegetation-period> [Accessed 30 April 2025].
- Sun, Y., Zhu, R., Wang, T. 2024. Projection of ex-

- treme climate change in the Asian arid region and the Tibetan Plateau in the early and middle 21st century based on NEX-GDDP-CMIP6. *Atmospheric and Oceanic Science Letters* 18(3), 100534. <https://doi.org/10.1016/j.aosl.2024.100534>
- Szyga-Pluta, K., Tomczyk, A.M., Piniewski, M., Eini, M.R. 2023. Past and future changes in the start, end, and duration of the growing season in Poland. *Acta Geophysica* 71(6), 3041–3055. <https://doi.org/10.1007/s11600-023-01117-1>
- Talchabhadel, R., Bhattarai, S., Bista, S. 2025. Projected Changes in Precipitation Extremes Across the Mississippi River Basin Using the NASA Global Daily Downscaled Datasets NEX-GDDP-CMIP6. *International Journal of Climatology* 45(5), e8748. <https://doi.org/10.1002/joc.8748>
- Thrasher, B., Maurer, E.P., McKellar, C., Duffy, P.B. 2012. Technical Note: Bias correcting climate model simulated daily temperature extremes with quantile mapping. *Hydrology and Earth System Sciences* 16(9), 3309–3314, <https://doi.org/10.5194/hess-16-3309-2012>
- Thrasher, B., Wang, W., Michaelis, A., Melton, F., Lee, T., Nemani, R. 2022. NASA Global Daily Downscaled Projections, CMIP6. *Scientific Data* 9(1), 1–6. <https://doi.org/10.1038/s41597-022-01393-4>
- Vautard, R., Van Oldenborgh, G.J., Bonnet, R., Li, S., Robin, Y., Kew, S., Philip, S., Soubeyroux, J.M., Dubuisson, B., Viovy, N., Reichstein, M., Otto, F., Garcia De Cortazar-Atauri, I. 2023. Human influence on growing-period frosts like in early April 2021 in central France. *Natural Hazards and Earth System Sciences* 23(3), 1045–1058. <https://doi.org/10.5194/nhess-23-1045-2023>
- Velikou, K., Lazoglou, G., Tolika, K., Anagnostopoulou, C. 2022. Reliability of the ERA5 in Replicating Mean and Extreme Temperatures across Europe. *Water (Switzerland)* 14(4). <https://doi.org/10.3390/w14040543>
- Vitasse, Y., Rebetez, M. 2018. Unprecedented risk of spring frost damage in Switzerland and Germany in 2017. *Climatic change* 149(2), 233–246. <https://doi.org/10.1007/s10584-018-2234-y>
- Wang, J., Guan, Y., Wu, L., Guan, X., Cai, W., Huang, J. 2021. Changing lengths of the four seasons by global warming. *Geophysical Research Letters* 48, e2020GL091753. <https://doi.org/10.1029/2020GL091753>
- Wang, T., Zhong, S., Andresen, J. 2025. Impacts of spring freeze events on a perennial tree fruit crop across the central and eastern USA. *International Journal of Biometeorology* 69, 1237–1252. <https://doi.org/10.1007/s00484-025-02887-7>
- Wypych, A., Sulikowska, A., Ustrnul, Z., Czekierda, D. 2017. Variability of growing degree days in Poland in response to ongoing climate changes in Europe. *International Journal of Biometeorology* 61(1), 49–59. <https://doi.org/10.1007/s00484-016-1190-3>
- Xia, J., Yan, Z., Jia, G., Zeng, H., Jones, P.D., Zhou, W., Zhang, A. 2015. Projections of the advance in the start of the growing season during the 21st century based on CMIP5 simulations. *Advances in Atmospheric Sciences* 32(6), 831–838. <https://doi.org/10.1007/s00376-014-4125-0>
- Xu, W., Lei, X., Chen, S., Yu, T., Hu, Z., Zhang, M., Jiang, L., Bao, R., Guan, X., Ma, M., Wei, J., Gao, L., Feng, A. 2022. How Well Does the ERA5 Reanalysis Capture the Extreme Climate Events Over China? Part II: Extreme Temperature. *Frontiers in Environmental Science* 10(June), 1–15. <https://doi.org/10.3389/fenvs.2022.921659>
- Zahradníček, P., Brázdil, R., Řehoř, J., Trnka, M., Bartošová, L., Rožnovský, J. 2024. Past and present risk of spring frosts for fruit trees in the Czech Republic. *Theoretical and Applied Climatology* 155(2), 965–984. <https://doi.org/10.1007/s00704-023-04671-2>
- Zhang, X., Huang, T., Wang, W., Shen, P. 2024. Change of global land extreme temperature in the future. *Global and Planetary Change* 242(September), 104583. <https://doi.org/10.1016/j.gloplacha.2024.104583>
- Zhu, L., Meng, J., Li, F., You, N. 2019. Predicting the patterns of change in spring onset and false springs in China during the twenty-first century. *International Journal of Biometeorology* 63(5), 591–606. <https://doi.org/10.1007/s00484-017-1456-4>
- Zscheischler, J., Raymond, C., Horton, R.M., Ramos, A.M. 2020. A typology of compound weather. *Nature Reviews Earth & Environment* 1, 333–347. <http://dx.doi.org/10.1038/s43017-020-0060-z>